Title

Placental glucose transporter 3 (GLUT3) is up-regulated in human pregnancies complicated by late-onset intrauterine growth restriction

Journal

Placenta, 34(11)

ISSN

0143-4004

Authors

Janzen, C
Lei, MYY
Cho, J
et al.

Publication Date

2013-11-01

DOI

10.1016/j.placenta.2013.08.010

Peer reviewed

Published in final edited form as:
Placenta. 2013 November ; 34(11): . doi:10.1016/j.placenta.2013.08.010.

Placental Glucose transporter 3 (GLUT3) is Up-regulated in Human Pregnancies Complicated by Late-onset Intrauterine Growth Restriction

Carla Janzen[1,*], **Margarida Y.Y. Lei**[1], **John Cho**[1], **Peggy Sullivan**[3], **Bo-Chul Shin**[2], and **Sherin U. Devaskar**[2]

[1]Department of Obstetrics and Gynecology/Division of Perinatology, David Geffen School of Medicine at UCLA, Los Angeles, CA 90095

[2]Department of Pediatrics/Neonatology & Developmental Biology, David Geffen School of Medicine at UCLA, Los Angeles, CA 90095

[3]Department of Pathology, David Geffen School of Medicine at UCLA, Los Angeles, CA 90095

Abstract

Introduction—Transport of glucose from maternal blood across the placental trophoblastic tissue barrier is critical to sustain fetal growth. The mechanism by which GLUTs are regulated in trophoblasts in response to ischemic hypoxia encountered with intra-uterine fetal growth restriction (IUGR) has not been suitably investigated.

Objective—To investigate placental expression of GLUT1, GLUT3 and GLUT4 and possible mechanisms of GLUT regulation in idiopathic IUGR.

Methods—We analyzed clinical, biochemical and histological data from placentas collected from women affected by idiopathic full-term IUGR (n=10) and gestational age-matched healthy controls (n=10).

Results—We found increased GLUT3 protein expression in the trophoblast (cytotrophoblast greater than syncytiotrophoblast) on the maternal aspect of the placenta in IUGR compared to normal placenta, but no differences in GLUT1 or GLUT4 were found. No differential methylation of the GLUT3 promoter between normal and IUGR placentas was observed. Increased GLUT3 expression was associated with an increased nuclear concentration of HIF-1α, suggesting hypoxia may play a role in the up-regulation of GLUT3.

Discussion—Further studies are needed to elucidate whether increased GLUT3 expression in IUGR is a marker for defective villous maturation or an adaptive response of the trophoblast in response to chronic hypoxia.

Conclusions—Patients with IUGR have increased trophoblast expression of GLUT3, as found under the low-oxygen conditions of the first trimester.

[*]Address all correspondence and reprint requests to: Carla Janzen, Department of Obstetrics and Gynecology, David Geffen School of Medicine at UCLA, 10833 Le Conte Avenue, Los Angeles, CA 90095-6928, USA, Tel: (310-206-6766); Fax: (310) 206-2057; cjanzen@mednet.ucla.edu.

DISCLOSURE STATEMENT: The authors have nothing to disclose

Key Terms

GLUT; Glucose; transport; Intrauterine growth restriction; Placenta

INTRODUCTION

Altered placental glucose transport due to chronic hypoxia may play a critical role in the pathophysiological events causing fetal intrauterine growth restriction (IUGR), a condition linked to increased newborn mortality and adult onset of chronic diseases such as diabetes and cancer [1, 2]. Glucose, which is essential for oxidative metabolism in the growing placenta and fetus, is transferred from maternal blood by facilitated carrier-mediated diffusion via glucose transporters. There are 14 known isoforms of the membrane-spanning glucose transporter family (the GLUTs), which are responsible for facilitated diffusion of glucose across the lipid bilayers of cell membranes [3]. The transporting epithelium of the human placental trophoblast expresses key members of the GLUT family including GLUT1 [4, 5], GLUT3 [6–8], and GLUT4 [9]. GLUT1, the main isoform expressed in mammalian placental syncytium, is found in high concentrations throughout pregnancy [10]. GLUT3 has both a higher affinity for glucose and a greater transport capacity than GLUT1 and GLUT4 [3]. Thus, GLUT3 is generally found in tissues that have a high rate of metabolic activity, such as neurons [11] and trophectoderm in pre-implantation embryos [12]. GLUT4 is distinguished as an insulin-sensitive isoform, which may mediate insulin-stimulated placental glucose uptake in early pregnancy [9]. The mechanism by which GLUTs are regulated in trophoblast in response to ischemic hypoxia has not been suitably investigated.

With the creation of a *Glut3*-null (*Glut3* $^{-/-}$) mouse model, it has definitively been shown that decreased GLUT3-mediated placental glucose transport causes late-gestation fetal growth restriction in *Glut3* heterozygous (*Glut3* $^{-/+}$) embryos. Growth restricted pups due to *Glut3* placental heterozygosity demonstrated catch-up growth after birth, similar to the pattern of growth seen in human late-onset IUGR [12]. In contrast, it is estimated that only 2 percent of structurally normal, growth-restricted human fetuses have a chromosomal abnormality and only 10% of IUGR in the Western world is attributable to nutritional deprivation as a primary cause [13]. The majority of pregnancies affected by late-onset IUGR are cases most likely attributable to ischemic placental disease that leads to disturbances in utero-placental flow causing chronic placental hypoxia [14, 15].

Studies of placental GLUT expression in human pregnancy affected by IUGR have been conflicting. Several *in-vivo* studies have not demonstrated differential placental GLUT expression in IUGR [16, 17]. In conditions of *in-vivo* chronic hypoxia, the expression of GLUT1 in the syncytium from the placentas of women living at high altitude was decreased by ~40% [18]. However, when maintained in hypoxic conditions *in-vitro*, trophoblasts isolated from term placenta demonstrated increased *GLUT1* and *GLUT3* mRNA [19]. In other *in-vitro* studies using BeWo, a trophoblast-derived choriocarcinoma cell line, reduction in oxygen tension led to dose-dependent increases in GLUT1 and GLUT3 expression and to increased transepithelial glucose transport [20, 21]. Up-regulation of GLUT1 and GLUT3 in these cells under hypoxic conditions was mechanistically demonstrated to be mediated by the hypoxia-inducible transcription factor-1α (HIF-1α).

It is reasonable to hypothesize that GLUT expression is up-regulated by hypoxia in the placental trophoblast *in-vivo* given that HIF-1α plays an essential role in adapting the cellular environment to hypoxic stress by inducing the expression of the GLUT family in numerous other tissues [22–25]. Increased placental transport of glucose in hypoxic conditions would potentially increase the concentration of glucose as an alternate metabolic

fuel to both the placenta and fetus, in which gluconeogenesis is limited [26]. However in the human, the fetus affected by IUGR demonstrates hypoglycemia, the magnitude of which is correlated to the severity of growth restriction [27] and magnitude of decreased blood flow [28]. It is thus widely believed that in conditions of fetal hypoxia leading to IUGR, it is an excess consumption of glucose by the placenta that is responsible for a decreased rate of transplacental transport to the fetus [29, 30].

Interestingly, HIF-1α is significantly increased in placenta from preeclamptic pregnancy [31]. Although late-term IUGR is thought to share the same placental etiology as preeclampsia, i.e., inadequate trophoblastic invasion leading to reduced uteroplacental perfusion and hypoxia, there was not an overall increased protein abundance of HIF-1α in placentas of late-term IUGR [32]. The extended explanation for these observations was that in pregnancy affected by IUGR, the growth-restricted fetus and placenta might display decreased oxygen consumption that offsets increases in hypoxia and HIF-1α signaling.

We hypothesized that stimulation of placental glucose transporter expression is an adaptive response to decreased uteroplacental perfusion and prolonged exposure to hypoxia, which is associated with late-term IUGR. To test this hypothesis, we investigated placental expression of GLUT1, GLUT3 and GLUT4 in the fetal vs. maternal aspect of placenta obtained from normotensive women who delivered growth-restricted babies at term (idiopathic IUGR) and possible mechanisms of placental GLUT regulation.

METHODS

Placental collection and processing

Informed consent under the approval of the UCLA IRB was obtained from women with normal pregnancy (n= 10), late-onset IUGR (n= 10), and preeclamptic pregnancies (n= 5). Clinical information for the groups is shown in Tables 1 and 2. IUGR was defined by newborn weight below or at the 10^{th} percentile for their gestational age and a demonstrated trajectory of fetal growth deceleration in utero, diagnosed by prenatal ultrasound [33]. 5 out of 10 IUGR babies were asymmetrically grown (Table 2). Asymmetric IUGR was defined by birth weight < length ≤ head circumference percentiles when the weight percentile was two percentile categories below length and/or head circumference as described previously [32]. The diagnosis of preeclampsia was made based on the Working Group Report on High Blood Pressure in Pregnancy [34]. Expression of hypoxia-related genes in the term placenta has been found to be dependent on the sampling site within the placental disk, with increased expression of VEGF and other transcripts occurring close to the lateral chorionic plate, the site of greatest hypo-perfusion [35]. We therefore separated our placental biopsies according to proximity to the chorionic plate as follows; using sterile technique, we cut a triangular segment of the placenta, with its convex base at the lateral edge of the placenta and its apex at the placental center near the cord insertion site. This triangular segment was then divided into 2 horizontal segments, with the basal plate on the bottom (maternal side) and the chorionic surface on the top (fetal side). Both the decidual layer along the basal plate as well as the chorionic surface and membranes were removed by sharp dissection and placental fragments were obtained at the middle of the initial placental depth, approximately 10 mm from the basal and chorionic plates.

Quantitative Real-Time PCR

Placental total RNA was extracted using Direct-zol RNA MiniPrep kit (Zymo Research, CA). First-strand cDNA was synthesized from 0.5 ug of DNase-treated total RNA using qScrip cDNA Synthesis Kit (Quanta Biosciences, MD) as previously described [36]. Primers and Taqman probes for detection of *GLUT1*, *GLUT3*, and *GLUT4* (GenBank accession nos.

NM_006516.2, NM_006931.2, and NM_001042.2); were designed using Primer Express (Applied Biosystems, CA). Primers used for *GLUT1*(71bp product), were 5′-atggcgggttgtgccata - 3′ (forward), 5′–ataggacatccagggtagctgctcc- 3′ (reverse), and 5′ –[6-FAM]tcatgaccatcgcgctagcactg[TAMRA-6-FAM]-3′ (probe), for GLUT3 (67bp product), were 5′ –caggcacacggtgcagatag - 3′ (forward), 5′-gcaggctcgatgctgttcat- 3′ (reverse), and 5′ –[6-FAM]tctggaaaggacggcgtcatgga[TAMRA-6-FAM] - 3′ (probe), for GLUT4 (68bp product), were 5′–ctgccagaaagagtctgaagc- 3′ (forward), 5′ –ccttcagctcagccagcact- 3′ (reverse), and 5′–[6-FAM]tgacaggctgggccgatgtttctg[TAMRA-6-FAM]- 3′ (probe).

Protein extraction

Placental tissues were homogenized and cell lysates were centrifuged for 15 minutes at 14,000xg and supernatants were collected for immunoblot analysis. Nuclear proteins were isolated using Qproteome Nuclear Protein Kit (Qiagen, CA).

Western blot analysis

Proteins were denatured and separated by SDS-PAGE using 10% TGX gels and transferred to PVDF membranes. Blots were probed in the following primary antibodies: rabbit-polyclonal for GLUT1 (Santa Cruz), GLUT4 (ABcam) HIF-1α (Cell Signaling), and mouse monoclonal for GLUT3 (Santa Cruz). Vinculin (Sigma, CA), beta actin (Cell Signaling) or Lamin A (ABcam) were used for loading controls. The blots were incubated with a secondary antibody using IgG-HRP and immunoreactive signals were analyzed using Pierce ECL Plus on a Typhoon Scanner 9410 through ImageQuant 5.2 software.

GLUT3 Promoter Methylation

Genomic DNA was extracted from placental tissue using QIAmp DNA mini kit (Qiagen). CpG islands present in *GLUT3* promoter regions were subjected to bisulfite modification. DNA methylation was quantified by pyrosequencing, as previously described [37]. The methylation status of each locus was analyzed individually as T/C SNP in QCpG software (Biotage AB).

Immunohistochemistry

Central full-thickness placental samples were embedded in paraffin blocks and mounted onto slides. The slides were deparaffinized in xylene and rehydrated in a graded series of ethanol and treated with methanol and hydrogen peroxide, and then incubated with Proteinase K (Dako, CA). Slides were incubated in rabbit-polyclonal antibodies for GLUT3 (IBL-America, MN), then incubated in EnVision and System-HRP (Dako, CA).

Immunohistochemistry image analysis

Digital images of GLUT3-stained slides were captured using the Keyence BZ-9000 Biorevo all-in-one microscope. Microscopic digital images of all fields on each section were scanned in frames composed of a 500-μm × 380-μm rectangles, and the area of GLUT3-positive cells in each rectangle were counted using software Dynamiccellcount BZ-HIC.

Localization of GLUT3 and HIF-1α

Placental slides were incubated for double staining with a mixture of primary antibodies, 1:100 dilution of rabbit anti-human GLUT3 (IBL, Minneapolis, MN) and 1:100 (Fig. 4D) or 1:50 (Fig. 4E) dilution of mouse anti-human HIF-1α (BD Biosciences, San Jose, CA) at roomtemperature for 2 hours, followed by overnight incubation at 4°C. Negative control consisted of absent primary antibody. Sections were washed thoroughly with 1x PBS and incubated with a mixture of 1:500 dilution of FITC -conjugated donkey anti-mouse, Texas red-conjugated donkey anti-rabbit secondary antibody (Jackson Immunoresearch, West

Grove, PA), and 1:1000 DAPI antibody (Sigma, St. Louis, MO) at room temperature for 1 hour. The sections were then examined under a fluorescence microscope at 40x magnification.

Data Analysis

Data are presented as mean ± SEM. After confirming that the data followed the normal distribution, means were compared using a 2 × 2 mixed effect analysis of variance (ANOVA) model with one between group effect (control, IUGR) and one within placental side effect (maternal side, fetal side). Results were considered statistically significant if $p < 0.05$. Computations were carried out using StatView 5.0 and JMP 10.0 (SAS Inc, Cary NC).

RESULTS

The expression of GLUT1, GLUT3 and GLUT4 in the fetal and maternal aspects of placenta from IUGR-affected pregnancy vs. control is shown in Figure 1. Figure 1A shows target genes that were quantified by quantitative real-time PCR with sequence-specific oligonucleotides. *GLUT3* mRNA increased in IUGR vs. control on the maternal aspect of the placenta and there was an increase of *GLUT4* mRNA concentration on the fetal aspect of the placenta. In contrast, there was a decrease of *GLUT1* mRNA concentration of the maternal region. Figure 1B demonstrates that by western blot, there was a 12% increase of GLUT3 protein expression on the maternal aspect of the IUGR placenta paralleling the corresponding mRNA increase, with no changes in GLUT1 and GLUT4. A 4-fold increase of placental GLUT3 protein expression was found when IUGR samples were analyzed by immunohistochemistry (Fig. 4C). These results suggest that only increased concentrations of *GLUT3* mRNA resulted in a corresponding increase in translated protein. We therefore focused further study on GLUT3.

Since uteroplacental insufficiency is a well-known risk factor for diminished oxygen supply to the fetus, we investigated the placental expression of HIF-1α, a major regulator of gene expression, including *GLUT3,* in other tissues under hypoxic conditions [22–25]. For this analysis, placentas were obtained from preeclamptic pregnancies as a positive control, since it has been documented that HIF-1α expression is significantly increased in preeclamptic placentas relative to normal placenta [31]. Figure 2A shows that concentrations of HIF-1α were significantly increased by western blot analysis within total cell proteins (whole cell lysate) on both the maternal and fetal aspects of the placenta in preeclamptic placentas (our positive control) relative to IUGR placentas. Since activation of HIF-1α leads to HIF-1α stabilization and nuclear translocation in conditions of hypoxia, we also analyzed the isolated nuclear fraction from our placental samples. Figure 2B demonstrates an increase in expression of HIF-1α within the nuclear fraction, not only in our positive control (preeclampsia), but also in the maternal aspect of the IUGR placentas, when compared to control. This result is consistent with activation of the HIF complex in the maternal aspect of the IUGR placenta.

To further investigate the mechanism by which GLUT3 expression is regulated in IUGR, we examined DNA methylation of the 5′–flanking region responsible for transcriptional regulation. By using gene specific primers, C to T conversion of CpG islands was assessed in the GLUT3 gene; CpG islands within 3 specified regions of the GLUT3 promoter demonstrated no differential methylation between normal and IUGR (Fig. 3).

Figure 4A shows a positive immunoreaction for GLUT3 in the maturing secondary spermatocytes adjacent to the lumen of the seminiferous tubule and sperm in our positive control. Negative control slides treated with bovine serum instead of primary antibody were negative (Fig. 4A). Figure 4B demonstrates immunohistochemical staining of slides

obtained from three different control placentas (top row, slides 1–3) adjacent to three different IUGR-affected placentas (bottom row, slides 4–6). GLUT3 positive immunoreactivity (brown) was seen in both the cytotrophoblast and syncytiotrophoblast (cytotrophoblast with greater staining than syncytiotrophoblast), (Fig. 4B and Fig. 4D1,5). IUGR placentas were notable for increased matrix-type fibrinoid deposition [38] and variable expression of GLUT3, with some terminal and intermediate villi staining positive, and adjacent villi of the same size remaining unlabeled. Placental tissue was analyzed for the overall level of GLUT3 expression by quantifying the GLUT3 positive staining area per squared micrometers on each slide objectively using Dynamiccellcount BZ-HIC software. This digital analysis revealed increased GLUT3 immunopositivity in IUGR as compared to normal placenta despite variable expression (Fig 4C). Placental sections reveal high expression of GLUT3 in extravillous trophoblasts embedded in fibrinoid matrix (Fig. 4B, 6). Figure 4D shows double immunolocalization of GLUT3 and HIF-1α. GLUT3 protein expression (red) was detected in both the cytotrophoblast and syncytiotrophoblast, again with variable expression from villi to villi. Similarly, HIF-1α (green) immunoreaction was found to have a pattern of distribution that was associated with GLUT3 trophoblast expression (yellow). This result is consistent with expression of GLUT3 in association with the activation of the HIF-1α complex in the placenta. Figure 4E demonstrates HIF-1α localization in a normal placenta (Fig. 4E, 1), the fetal aspect of an IUGR placenta (Fig. 4E, 2) and the maternal aspect of the same IUGR placenta (Fig. 4E, 3). HIF-1α nuclear localization is appreciated to the greatest extent in the maternal aspect of IUGR (Fig. 4E, 3).

DISCUSSION

We found increased GLUT3 protein in the maternal aspect of the placenta and no difference in GLUT1 and GLUT4 proteins in pregnancy affected by idiopathic late-term IUGR as compared to normal pregnancy. Increased placental GLUT3 was associated with increased activation of placental HIF-1α, suggesting that hypoxia may play a role in up-regulation of GLUT3. GLUT3 immunolocalized in the cytotrophoblast and syncytiotrophoblast, with a heterogeneous distribution pattern similar to that of GLUT3 mRNA described by Hauguel-De Mouzon, *et. al.* in normal term placenta [8]. The variable presence of GLUT3 may serve as a marker for differential ischemic hypoxia in certain villi, not being present in others.

Variable expression of GLUT3 protein is likely attributable to several factors. First, placental lesions of IUGR are related to underperfusion due to varying pathologies such as poor uteroplacental blood flow due to maternal vascular disease, decreased elaboration of terminal villi owing to abnormal fetoplacental angiogenesis, and chronic villitis [39–41]. The extent of placental damage is related to impaired fetal growth as evolving placental injury leads to compromise of placental gas exchange, causing progressive fetal hypoxia [42]. With damage to the trophoblast, there is an increased local activation of the coagulation cascade in the inter-villous space causing excessive deposition of perivillous fibrin. Indeed, the IUGR placentas we obtained in this study were notable for increased fibrinoid deposition. Fibrinoid embeds placental villi, causing impaired transplacental gas and nutrient exchange. Interestingly, we observed multiple examples of increased GLUT3 in the trophoblast of villi adjacent to fibrinoid deposition by immunohistochemistry in both normal placenta and placenta affected by IUGR or preeclampsia. We thus speculate that regional perfusion differences in the placenta initiate a cascade of increased fibrinoid deposition, hypoxia, and ultimately increased trophoblast expression of GLUT3 regionally by activation of HIF-1α. It is likely that increased expression of GLUT3, specifically on the maternal aspect of the placenta, is caused by accumulation of perivillous fibrinoid extending from the basal plate, where primary maternal vascular lesions limit perfusion to the intervillous space.

In this study, GLUT3 was expressed by the cytotrophoblast, and to a lesser degree, the syncytiotrophoblast. Syncytiotrophoblast GLUT3 expression is not surprising given that in placentas derived from mice, rats and sheep, GLUT3 expression is seen in maternal-facing syncytiotrophoblast cells (STBs) that form the labyrinthine region responsible for materno-fetal transfer of glucose. A finding of this study that may further explain variable expression of GLUT3 was the high degree of GLUT3 localization in the term placentalcytotrophoblast cells (CTBs). This is similar to the findings of multiple investigators who have observed GLUT3 expression exclusively in the CTBs of human placenta in early pregnancy [43–45]. CTBs contain stem cells, which differentiate to become non-proliferative multinucleated STBs with cell fusion. A hypothesis for the reduction of GLUT3 with advancing gestation is that with extensive differentiation to STBs, there is cessation of active division of CTB stem cells and therefore decreased metabolic activity; in other words, GLUT3, which is highly associated with tissues that have a high rate of metabolic activity such as dividing CTBs, is no longer required to the same extent in the differentiated STB [46]. In 1997, Clarson *et. al.* hypothesized that the reason for contrasting reports regarding the detection of GLUT3 protein in the human placenta may be due to GLUT3 expression that is exclusive to the small sub-population of CTBs that are still dividing in late gestation [46]. Future studies will address the question of whether increased GLUT3 expression in term placentas associated with IUGR may signify an adaptive deceleration of placental development to accommodate and survive the ischemic-hypoxic environment.

The physiological impact of increased GLUT3 expression in IUGR placenta on the flux of glucose from the maternal to fetal circulation is unclear. It is possible that increased GLUT3 expression within late-term IUGR CTB may represent a mechanism by which the placenta attempts to increase glucose transport from the STB to the fetal circulation as an alternative fuel in a hypoxic environment. Observed increasing fetal hypoglycemia, the magnitude of which is correlated to the severity of IUGR [27] and magnitude of decreased blood flow [28], may suggest that this mechanism backfires. Increased GLUT3 within late-term IUGR CTB could plausibly lead to a reversal of transplacental glucose flux resulting in transport from the fetus into the placental tissue, as has been described with maternal hypoglycemia [47]. More likely, increased GLUT3 within late-term IUGR CTB helps supply an excess consumption of glucose by the placenta itself, leading to a decreased rate of transplacental transport to the fetus [29, 30].

Conclusions

We found that GLUT3 protein expression was increased in the maternal aspect of the placenta in idiopathic IUGR. Increased GLUT3 expression was associated with an increased nuclear concentration of HIF-1α, suggesting that chronic hypoxia may play a role in GLUT3 up-regulation. This finding suggests that with utero-placental vascular insufficiency, rather than down-regulating GLUT3 expression as seen with normal term placenta, there is continued CTB expression of GLUT3, as found under the low-oxygen conditions of the first trimester. Further studies are needed to elucidate whether increased GLUT3 expression in IUGR is a marker for stem cells with a proliferative capacity resulting in defective villous maturation or an adaptive re-setting of the epithelial cell in response to various stimuli.

Acknowledgments

We warmly thank Jeffrey A. Gornbeinfor his biostatistical assistance and Sanjali Kumar for her technical assistance.

This work was supported by K12 WRHR HD-001281 (CJ). Bo-Chul Shin is supported by NIH HD25024 and Sherin U. Devaskar is supported by NIH HD-46979, HD-33997, HD-41230 & HD-25024 (to SUD) and the National Center for Advancing Translational Sciences through UCLA CTSI Grant UL1TR000124 (to SUD).

References

1. Barker DJ, Osmond C, Forsen TJ, Kajantie E, Eriksson JG. Trajectories of growth among children who have coronary events as adults. The New England journal of medicine. 2005; 353(17):1802–9. [PubMed: 16251536]
2. Burdge GC, Lillycrop KA, Jackson AA. Nutrition in early life, and risk of cancer and metabolic disease: alternative endings in an epigenetic tale? The British journal of nutrition. 2009; 101(5): 619–30. [PubMed: 19079817]
3. Simpson IA, Dwyer D, Malide D, Moley KH, Travis A, Vannucci SJ. The facilitative glucose transporter GLUT3: 20 years of distinction. American journal of physiology Endocrinology and metabolism. 2008; 295(2):E242–53. [PubMed: 18577699]
4. Takata K, Kasahara T, Kasahara M, Ezaki O, Hirano H. Erythrocyte/HepG2-type glucose transporter is concentrated in cells of blood-tissue barriers. Biochemical and biophysical research communications. 1990; 173(1):67–73. [PubMed: 2256938]
5. Devaskar SU, Mueckler MM. The mammalian glucose transporters. Pediatric research. 1992; 31(1): 1–13. [PubMed: 1594323]
6. Kayano T, Fukumoto H, Eddy RL, Fan YS, Byers MG, Shows TB, Bell GI. Evidence for a family of human glucose transporter-like proteins. Sequence and gene localization of a protein expressed in fetal skeletal muscle and other tissues. The Journal of biological chemistry. 1988; 263(30):15245–8. [PubMed: 3170580]
7. Brown K, Heller DS, Zamudio S, Illsley NP. Glucose transporter 3 (GLUT3) protein expression in human placenta across gestation. Placenta. 32(12):1041–9. [PubMed: 22000473]
8. Hauguel-de Mouzon S, Challier JC, Kacemi A, Cauzac M, Malek A, Girard J. The GLUT3 glucose transporter isoform is differentially expressed within human placental cell types. The Journal of clinical endocrinology and metabolism. 1997; 82(8):2689–94. [PubMed: 9253355]
9. Ericsson A, Hamark B, Powell TL, Jansson T. Glucose transporter isoform 4 is expressed in the syncytiotrophoblast of first trimester human placenta. Hum Reprod. 2005; 20(2):521–30. [PubMed: 15528266]
10. Sakata M, Kurachi H, Imai T, Tadokoro C, Yamaguchi M, Yoshimoto Y, Oka Y, Miyake A. Increase in human placental glucose transporter-1 during pregnancy. European journal of endocrinology/European Federation of Endocrine Societies. 1995; 132(2):206–12. [PubMed: 7858740]
11. Mantych GJ, James DE, Chung HD, Devaskar SU. Cellular localization and characterization of Glut 3 glucose transporter isoform in human brain. Endocrinology. 1992; 131(3):1270–8. [PubMed: 1505464]
12. Ganguly A, McKnight RA, Raychaudhuri S, Shin BC, Ma Z, Moley K, Devaskar SU. Glucose transporter isoform-3 mutations cause early pregnancy loss and fetal growth restriction. American journal of physiology Endocrinology and metabolism. 2007; 292(5):E1241–55. [PubMed: 17213475]
13. Berghella V. Prevention of recurrent fetal growth restriction. Obstetrics and gynecology. 2007; 110(4):904–12. [PubMed: 17906027]
14. Redline RW. Placental pathology: a systematic approach with clinical correlations. Placenta. 2008; 29 (Suppl A):S86–91. [PubMed: 17950457]
15. Ghidini A. Idiopathic fetal growth restriction: a pathophysiologic approach. Obstetrical & gynecological survey. 1996; 51(6):376–82. [PubMed: 8771577]
16. Jansson T, Ylven K, Wennergren M, Powell TL. Glucose transport and system A activity in syncytiotrophoblast microvillous and basal plasma membranes in intrauterine growth restriction. Placenta. 2002; 23(5):392–9. [PubMed: 12061855]
17. Kainulainen H, Jarvinen T, Heinonen PK. Placental glucose transporters in fetal intrauterine growth retardation and macrosomia. Gynecologic and obstetric investigation. 1997; 44(2):89–92. [PubMed: 9286719]
18. Zamudio S, Baumann MU, Illsley NP. Effects of chronic hypoxia in vivo on the expression of human placental glucose transporters. Placenta. 2006; 27(1):49–55. [PubMed: 16310037]

19. Esterman A, Greco MA, Mitani Y, Finlay TH, Ismail-Beigi F, Dancis J. The effect of hypoxia on human trophoblast in culture: morphology, glucose transport and metabolism. Placenta. 1997; 18(2–3):129–36. [PubMed: 9089773]

20. Baumann MU, Zamudio S, Illsley NP. Hypoxic upregulation of glucose transporters in BeWo choriocarcinoma cells is mediated by hypoxia-inducible factor-1. Am J Physiol Cell Physiol. 2007; 293(1):C477–85. [PubMed: 17442736]

21. Hayashi M, Sakata M, Takeda T, Yamamoto T, Okamoto Y, Sawada K, Kimura A, Minekawa R, Tahara M, Tasaka K, Murata Y. Induction of glucose transporter 1 expression through hypoxia-inducible factor 1alpha under hypoxic conditions in trophoblast-derived cells. J Endocrinol. 2004; 183(1):145–54. [PubMed: 15525582]

22. Yu J, Li J, Zhang S, Xu X, Zheng M, Jiang G, Li F. IGF-1 induces hypoxia-inducible factor 1alpha-mediated GLUT3 expression through PI3K/Akt/mTOR dependent pathways in PC12 cells. Brain research. 2012; 1430:18–24. [PubMed: 22104347]

23. Gleadle JM, Ratcliffe PJ. Induction of hypoxia-inducible factor-1, erythropoietin, vascular endothelial growth factor, and glucose transporter-1 by hypoxia: evidence against a regulatory role for Src kinase. Blood. 1997; 89(2):503–9. [PubMed: 9002952]

24. Denko NC. Hypoxia, HIF1 and glucose metabolism in the solid tumour. Nature reviews Cancer. 2008; 8(9):705–13.

25. Iyer NV, Kotch LE, Agani F, Leung SW, Laughner E, Wenger RH, Gassmann M, Gearhart JD, Lawler AM, Yu AY, Semenza GL. Cellular and developmental control of O2 homeostasis by hypoxia-inducible factor 1 alpha. Genes & development. 1998; 12(2):149–62. [PubMed: 9436976]

26. Marconi AM, Cetin I, Davoli E, Baggiani AM, Fanelli R, Fennessey PV, Battaglia FC, Pardi G. An evaluation of fetal glucogenesis in intrauterine growth-retarded pregnancies. Metabolism: clinical and experimental. 1993; 42(7):860–4. [PubMed: 8345796]

27. Marconi AM, Paolini CL. Nutrient transport across the intrauterine growth-restricted placenta. Seminars in perinatology. 2008; 32(3):178–81. [PubMed: 18482618]

28. Economides DL, Nicolaides KH, Campbell S. Relation between maternal-to-fetal blood glucose gradient and uterine and umbilical Doppler blood flow measurements. British journal of obstetrics and gynaecology. 1990; 97(6):543–4. [PubMed: 2198923]

29. Challis DE, Pfarrer CD, Ritchie JW, Koren G, Adamson SL. Glucose metabolism is elevated and vascular resistance and maternofetal transfer is normal in perfused placental cotyledons from severely growth-restricted fetuses. Pediatric research. 2000; 47(3):309–15. [PubMed: 10709728]

30. Zamudio S, Torricos T, Fik E, Oyala M, Echalar L, Pullockaran J, Tutino E, Martin B, Belliappa S, Balanza E, Illsley NP. Hypoglycemia and the origin of hypoxia-induced reduction in human fetal growth. PloS one. 2010; 5(1):e8551. [PubMed: 20049329]

31. Rajakumar A, Brandon HM, Daftary A, Ness R, Conrad KP. Evidence for the functional activity of hypoxia-inducible transcription factors overexpressed in preeclamptic placentae. Placenta. 2004; 25(10):763–9. [PubMed: 15451190]

32. Rajakumar A, Jeyabalan A, Markovic N, Ness R, Gilmour C, Conrad KP. Placental HIF-1 alpha, HIF-2 alpha, membrane and soluble VEGF receptor-1 proteins are not increased in normotensive pregnancies complicated by late-onset intrauterine growth restriction. American journal of physiology Regulatory, integrative and comparative physiology. 2007; 293(2):R766–74.

33. Boulet SL, Alexander GR, Salihu HM, Kirby RS, Carlo WA. Fetal growth risk curves: defining levels of fetal growth restriction by neonatal death risk. American journal of obstetrics and gynecology. 2006; 195(6):1571–7. [PubMed: 16769013]

34. Roberts JM, Pearson GD, Cutler JA, Lindheimer MD. Summary of the NHLBI Working Group on Research on Hypertension During Pregnancy. Hypertension in pregnancy: official journal of the International Society for the Study of Hypertension in Pregnancy. 2003; 22(2):109–27. [PubMed: 12908996]

35. Wyatt SM, Kraus FT, Roh CR, Elchalal U, Nelson DM, Sadovsky Y. The correlation between sampling site and gene expression in the term human placenta. Placenta. 2005; 26(5):372–9. [PubMed: 15850641]

36. Thamotharan M, Shin BC, Suddirikku DT, Thamotharan S, Garg M, Devaskar SU. GLUT4 expression and subcellular localization in the intrauterine growth-restricted adult rat female

offspring. American journal of physiology Endocrinology and metabolism. 2005; 288(5):E935–47. [PubMed: 15625086]

37. Shin BC, Dai Y, Thamotharan M, Gibson LC, Devaskar SU. Pre- and postnatal calorie restriction perturbs early hypothalamic neuropeptide and energy balance. Journal of neuroscience research. 2012; 90(6):1169–82. [PubMed: 22388752]
38. Huppertz B, Kertschanska S, Frank HG, Gaus G, Funayama H, Kaufmann P. Extracellular matrix components of the placental extravillous trophoblast: immunocytochemistry and ultrastructural distribution. Histochemistry and cell biology. 1996; 106(3):291–301. [PubMed: 8897070]
39. Viero S, Chaddha V, Alkazaleh F, Simchen MJ, Malik A, Kelly E, Windrim R, Kingdom JC. Prognostic value of placental ultrasound in pregnancies complicated by absent end-diastolic flow velocity in the umbilical arteries. Placenta. 2004; 25(8–9):735–41. [PubMed: 15450392]
40. Salafia CM, Charles AK, Maas EM. Placenta and fetal growth restriction. Clinical obstetrics and gynecology. 2006; 49(2):236–56. [PubMed: 16721104]
41. Greer LG, Ziadie MS, Casey BM, Rogers BB, McIntire DD, Leveno KJ. An immunologic basis for placental insufficiency in fetal growth restriction. American journal of perinatology. 2012; 29(7): 533–8. [PubMed: 22495894]
42. Salafia CM, Minior VK, Pezzullo JC, Popek EJ, Rosenkrantz TS, Vintzileos AM. Intrauterine growth restriction in infants of less than thirty-two weeks' gestation: associated placental pathologic features. American journal of obstetrics and gynecology. 1995; 173(4):1049–57. [PubMed: 7485292]
43. Tadokoro N, Koibuchi N, Ohtake H, Kawatsu T, Tanaka S, Ohkawa H, Kato Y, Yamaoka S, Kumasaka T. Localization of prolactin and its receptor messenger RNA in the human decidua. Experientia. 1995; 51(12):1216–9. [PubMed: 8536809]
44. Ogura K, Sakata M, Okamoto Y, Yasui Y, Tadokoro C, Yoshimoto Y, Yamaguchi M, Kurachi H, Maeda T, Murata Y. 8-bromo-cyclicAMP stimulates glucose transporter-1 expression in a human choriocarcinoma cell line. The Journal of endocrinology. 2000; 164(2):171–8. [PubMed: 10657852]
45. Sato M, Nakamura Y, Sogawa T, Yang Q, Taniguchi T, Taniguchi E, Kagiya T, Nakamura M, Mori I, Kakudo K. Immunolocalization of glucose transporter 1 and 3 in the placenta: application to cytodiagnosis of Papanicolaou smear. Diagnostic cytopathology. 2002; 26(6):373–9. [PubMed: 12112827]
46. Clarson LH, Glazier JD, Sides MK, Sibley CP. Expression of the facilitated glucose transporters (GLUT1 and GLUT3) by a choriocarcinoma cell line (JAr) and cytotrophoblast cells in culture. Placenta. 1997; 18(4):333–9. [PubMed: 9179927]
47. Schneider H, Reiber W, Sager R, Malek A. Asymmetrical transport of glucose across the in vitro perfused human placenta. Placenta. 2003; 24(1):27–33. [PubMed: 12495656]

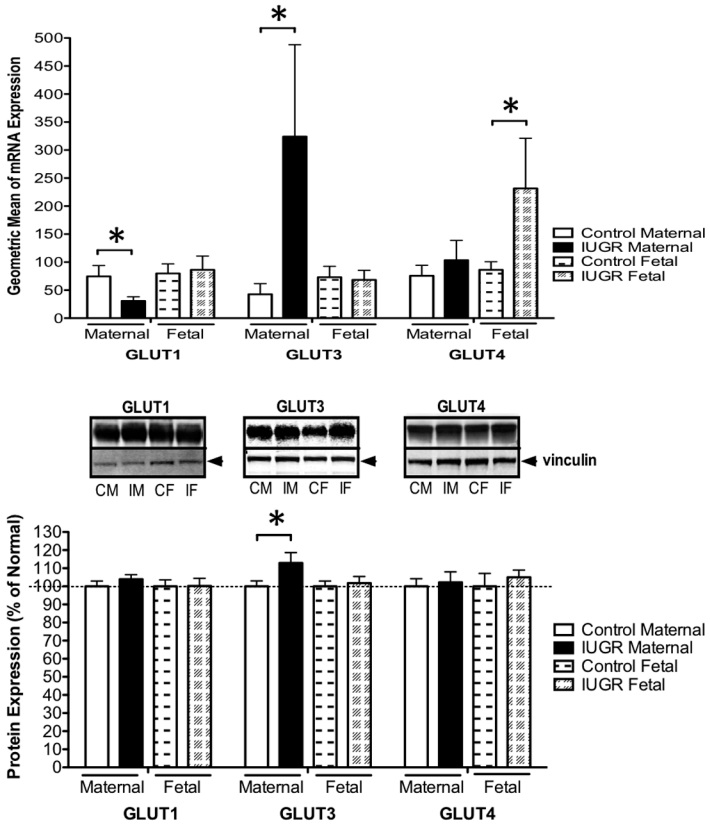

Fig. 1.

(A) Real-time quantitative RT-PCR analysis of placental *GLUT1*, *GLUT3* and *GLUT4* expression. IUGR placentas (n=10) are assayed against gestationally age-matched, control placentas (n=10) for the maternal vs. fetal side. Relative quantification of PCR products was based on the Ct value differences between target and the housekeeping gene using the comparative Ct method (Eukaryotic 18s rRNA (Applied Biosystems) was used as an internal control. *P < 0.05. (B) Western blot analysis of GLUT1, GLUT3, and GLUT4 in placental biopsies obtained from women with normal pregnancy (n=10) or pregnancy affected by IUGR, suspected by abnormal prenatal ultrasound (n=10). Protein taken from fetal (F) and maternal (M) sides were loaded on 12% SDS-polyacrylamide gels and transferred onto PVDF membranes. Representative blots are shown. (B, Bottom) Arbitrary densitometric units showing mean of all samples; data are normalized to a control value of 100%, bars indicate SE. *P < 0.05.

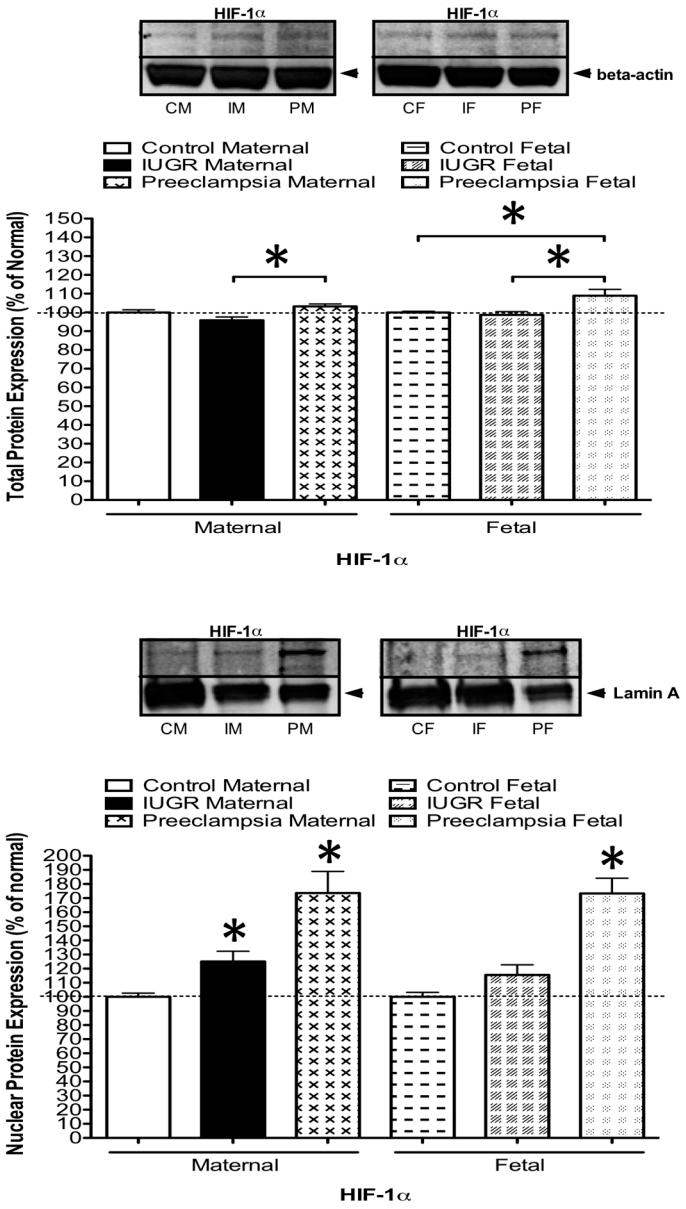

Fig. 2.

(A) Western blot analysis of HIF-1α in total protein of placental biopsies obtained from the maternal and fetal sides in women with normal pregnancy (n=10), or pregnancy affected by IUGR, suspected by abnormal prenatal ultrasound (n=10), or preeclampsia (n=5). Representative blots are shown. Arbitrary densitometric units showing mean of all samples; data are normalized to a control value of 100%, bars indicate SE. *P < 0.05 (B) Western blot analysis of HIF-1α in nuclear fraction of placental biopsies obtained from the maternal and fetal sides in women with normal pregnancy (n=10), or pregnancy affected by IUGR (n=10) or preeclampsia (n=5). Representative blots are shown. Arbitrary densitometric units showing mean of all samples; data are normalized to a control value of 100%, bars indicate SE. *P < 0.05

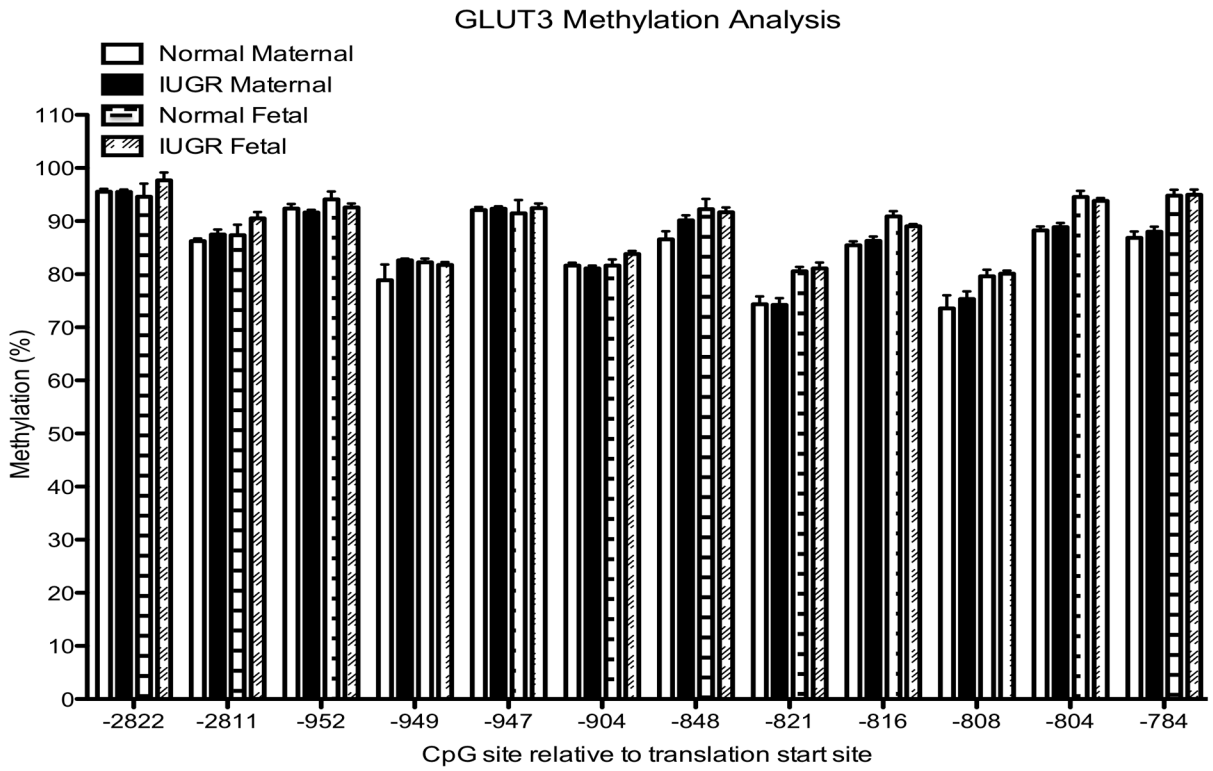

Fig. 3.

DNA methylation analysis of placental *GLUT3* promoter regions in placental biopsies obtained from the maternal and fetal sides in women with normal pregnancy and pregnancy affected by IUGR. Genomic DNA was processed by pyrosequencing.

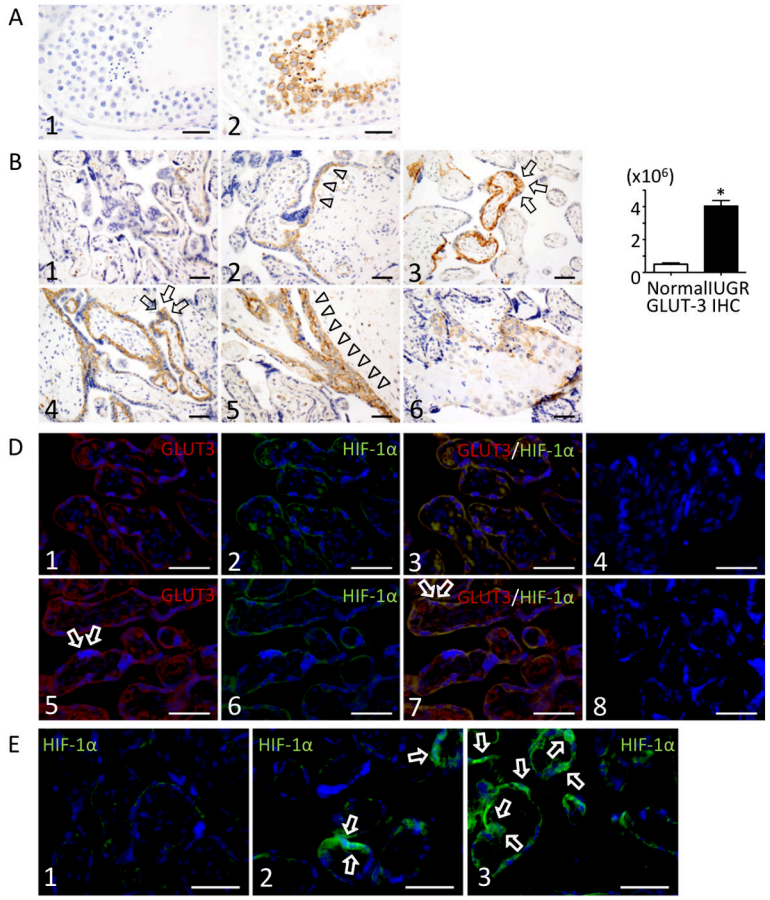

Fig. 4.

Immunohistochemical localization of GLUT3 and HIF-1α in human placenta. (A) Controls for GLUT3 staining at 600x magnification. GLUT3 staining of human testis; there was no GLUT3 staining in sections where the primary antibody was omitted (A1). Positive control (testis) shows immunoreaction for GLUT3 (brown) in the maturing secondary spermatocytes and sperm (A2). (B) Sections of three different subjects showing normal term placenta (B1-B3) vs. IUGR (slide B4=sample 8, slide B5=sample 10, slide B6=sample 5), stained with GLUT3, staining at 400x magnification. GLUT3 is localized to the cytotrophoblast layer and the syncytiotrophoblast layer to a lesser degree. Arrows indicate immunoreactive syncytium, as determined by their morphology and location relative to the intervillous space. Triangles show underlying cytotrophoblast layer. Scale bars = 50μm (C) GLUT3 positive staining area per squared micrometers was quantified using Dynamiccellcount BZ-HIC software. Digital analysis revealed increased GLUT3 immunopositivity in IUGR as compared to normal placenta. *P < 0.05 (D) Double immunohistochemical localization of GLUT3(red) and HIF -1α(green) in control placenta (slides D1-D4) and IUGR (slides D5-D8). D1 and D5: stained for GLUT3 (Texas Red) and DAPI (nuclear blue). D2 and D6: stained for HIF-1α (FITC green) and DAPI (nuclear blue). D3 and D7: triple stained for GLUT3 (Texas Red), HIF-1α (FITC green), and DAPI (nuclear blue). Arrows indicate immunoreactive syncytium, as determined by their morphology and location relative to the intervillous space. D4 and D8: negative controls performed by omission of primary antibody and showed that cross-staining did not occur. Scale bars = 50μm (E) HIF-1α (green) staining in normal placenta (E1) vs. IUGR, fetal

aspect (E2) vs. IUGR, maternal aspect (E3). Arrows indicate immunoreactive syncytium. Scale bars = 50μm.

Table 1

Clinical Characteristics of control group and cases

	Normal Pregnancy (n = 10)	IUGR (n = 10)	Preeclampsia (n = 5)
Maternal Age (years)	34.5±1.6	29.3±1.9	26.4±2.1
Gestational age at delivery (weeks)	38.96±0.3	38±0.4	36.9±0.9
Birth weight (g)	3448.1±92.7	2392.97±77.1§	2724.0±254.7
Placental weight (g)	622.9±46.7	480.0±46.6	598.2±80.8

Means ± SE.

§P<0.0001 vs. normal pregnancy.

Placenta. Author manuscript; available in PMC 2014 November 01.

Table 2

Clinical Characteristics of IUGR Pregnancies

	Birth Weight, g	Percentile (%)	Length (cm)	Percentile (%)	Head Circumference (cm)	Percentile (%)	Gestational Age (wk)	Growth Profile	Ultrasound findings	Clinical course
1	2475	8	48.3	45	33	30	37.6	*asymmetrical*	Fetal growth deceleration diagnosed at 37 weeks	Labor induction for uncomplicated fetal growth restriction
2	2239.7	3	46	10	31	7	37.7	*asymmetrical*	Fetal growth deceleration diagnosed at 35 weeks	NICU admission for neonatal hypoglycemia
	2551.5	7	49.5	50	33	20	38.6	*asymmetrical*	Fetal growth deceleration diagnosed at 37 weeks	NICU admission for neonatal hypoglycemia and hypothermia
	2190	3	47.3	15	30.5	3	37.9	*asymmetrical*	Fetal growth deceleration diagnosed at 34 weeks	Cesarean section for fetal distress, NICU admission for neonatal hypoglycemia
	2645	7	49	30	32.5	10	38.9	*asymmetrical*	Abnormal MCA Doppler exam with brain sparing effect, Fetal growth deceleration diagnosed at 38 weeks	
	2580	2	46.5	3	31	<3	40.4	symmetrical	Cesarean section for fetal distress	
	2608.2	7	44.5	<3	33	10	39	symmetrical	Fetal growth deceleration diagnosed at 35 weeks	
8	2320.3	9	45.3	10	32.3	25	36.7	symmetrical	Abnormal umbilical artery Doppler exam, Fetal growth deceleration diagnosed at 37 weeks	NICU admission for respiratory distress
9	2460	7	43.2	<3	30.5	3	37.9	symmetrical	Abnormal umbilical artery and MCA Doppler exam, Fetal growth deceleration diagnosed at 37 weeks	NICU admission for fetal hypothermia and hypoglycemia

	Birth Weight, g	Percentile (%)	Length (cm)	Percentile (%)	Head Circumference (cm)	Percentile (%)	Gestational Age (wk)	Growth Profile	Ultrasound findings	Clinical course
10	1860	7	44	10	29.9	9	35.3	symmetrical	Fetal growth deceleration diagnosed at 34 weeks Oligohydramnios	Labor induction for oligohydramnios NICU admission for respiratory distress